0026-895X/91/040584-07$03.00/0
Copyright © by The American Society for Pharmacology and Experimental Therapeutics
All rights of reproduction in any form reserved.
MOLECULAR PHARMACOLOGY, 40:584-590

MOL PHARM

Reversed Siderophores as Antimalarial Agents. II. Selective Scavenging of Fe(III) from Parasitized Erythrocytes by a Fluorescent Derivative of Desferal

SIMON D. LYTTON, Z. IOAV CABANTCHIK, JACQUELINE LIBMAN, and ABRAHAM SHANZER

Department of Biological Chemistry, Institute of Life Sciences, Hebrew University, Jerusalem, Israel 91904 (S.D.L., Z.I.C.), and Department of Organic Chemistry, Weizmann Institute of Science, Rehovot, Israel 76100 (J.L., A.S.)

Received April 12, 1991; Accepted June 24, 1991

SUMMARY

We introduce here a fluorescent derivative of desferrioxamine B (DFO) that retains the high affinity of the parent compound and displays a powerful inhibition of intraerythrocytic *Plasmodium falciparum* growth. NBD-DFO was synthesized by coupling 7-Nitrobenz-2-oxa-1,3-diazole (NBD) to the terminal amino group of DFO. The NBD group at this position renders the DFO molecule more lipophilic and imparts to it fluorescent properties. The novel NBD-DFO probe displays a unique combination of chemical and biological properties, such as 1) improved and selective permeation properties across membranes of *P. falciparum*-infected erythrocytes, 2) improved efficacy as an inhibitor of intraerythrocytic *P. falciparum* growth (including multidrug-resistant strains), 3) demonstrable Fe^{3+} scavenging within parasitized red cells, and 4) usefulness as a sensitive and versatile analytical tool for quantitative assessment of Fe^{3+} and for following iron-scavenging processes, because the fluorescence of NBD-DFO is demonstrably quenched upon complexation with Fe^{3+}.

Worldwide resurgence of malaria and the spread of strains of *Plasmodium falciparum* that are resistant to quinolines and antifolates, the drugs in most common use, have created an urgent need for new antimalarial agents (1, 2). Because the malaria parasite thrives inside host red cells, compounds that induce differential iron deprivation should prove to be useful antimalarial agents even against parasites of the most drug-resistant nature (2). This idea gained momentum when clinical observations suggested that iron metabolism and malaria infection are closely interrelated (3–6).

DFO, an iron-specific hydroxamate chelator, has been shown to suppress malaria infection *in vitro* (7, 8) and in several rodent and primate species *in vivo* (9–12). Although the drug has been in commercial use since the late 1960s to increase iron excretion and reduce iron overload (13–15), its poor absorption from the gastrointestinal trace, short serum half-time, requiring continuous parenteral administration for optimal effect (15, 16), toxic side effects (17, 18), and, in particular, very slow penetration into erythrocytes (19) have hampered its therapeutic use as an antimalarial agent. Several studies on desferal (11, 20) and hydroxamate-based "reversed siderophores" (21) showed that they act by scavenging a vital intraerythrocyte Fe(III) source, either degraded hemoglobin (22, 23) or essential enzymes (24) or putative parasite-derived iron carriers.

In order to overcome the major shortcoming of DFO, we aimed at a minimal modification of its structure that would selectively enhance permeation into parasitized erythrocytes, without affecting the Fe^{3+}-binding properties of the parent molecule. Because the terminal amino-group of DFO does not participate in iron binding *per se*, we modified DFO by coupling the hydrophobic fluorescent group NBD to the terminal amino-group of DFO, resulting in a probe (NBD-DFO) (Fig. 1) with novel features. These include increased hydrophobicity relative to DFO, reduced basicity under physiological conditions, and spectroscopic properties that allow tracing of Fe(III). The latter resulted from the fact that, upon stoichiometric binding of Fe(III), the NBD-DFO fluorescence was markedly quenched by the bound metal. Moreover, the specificity and high binding properties of DFO were fully retained in the NBD derivative. In this article, we demonstrate that the improved antimalarial activity of NBD-DFO resides in its selectively permeability into infected red cells, by virtue of its higher lipophilicity and capacity for chelating intracellular Fe(III). This mode of action is consistent with the concept of reversed siderophores introduced in our earlier report on synthetic ferrichromes (21), where their antimalarial activity was reported to be highly correlated with their membrane-permeation properties.

This work was supported in part by National Institutes of Health Grant AI23042 and AID-CDR C-241 (Z.I.C.).

ABBREVIATIONS: DFO, desferrioxamine; NBD, 7-nitrobenz-2-oxa-1,3-diazole; HEPES, 4-(2-hydroxyethyl)-1-piperazine-ethanesulfonic acid; DMSO, dimethylsulfoxide; TCA, trichloroacetic acid.

MOLECULAR PHARMACOLOGY
aspet
Downloaded from molpharm.aspetjournals.org at Universidade do Estado do Rio de Janeiro on December 4, 2012

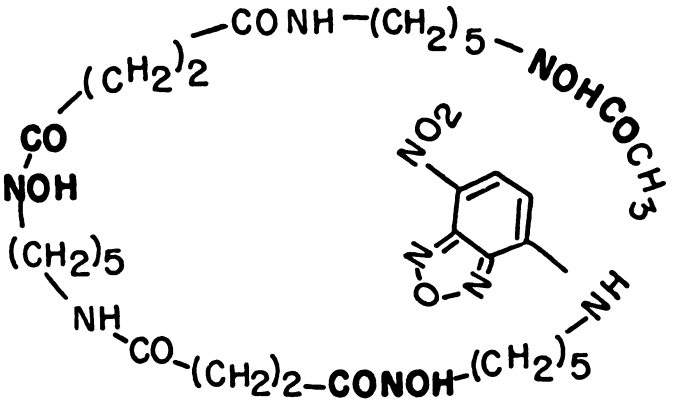

Fig. 1. Molecular structure of NBD-DFO.

Materials and Methods

Synthesis of NBD-DFO. The synthesis of NBD-DFO was performed according to a procedure used for the preparation of NBD-glycine (25). Briefly, to 656 mg (10^{-3} mol) of desferrioxamine B methylsulfonate (desferal), dissolved in 10 ml of methanol and 20 ml of 0.1 N aqueous $NaHCO_3$, were added 200 mg (10^{-3} mol) of NBD-Cl dissolved in 7.5 ml of methanol. The mixture was heated for 1 hr in an oil bath of 65°. The crude reaction mixture was concentrated *in vacuo* and chromatographed through a silica gel column (Woelm 63-100), using chloroform/methanol (9:1) as eluent, and 140 mg of NBD-DFO were collected and purified by crystallization from a mixture of methanol and acetonitrile. This material was characterized as follows: m.p. 131–133°; NMR (CD_3OD): δ 8.530 (d, J = 8.8 Hz, 1 H, Ar-H), 6.361 (d, J = 8.9 Hz, 1 H, Ar-H), 3.57 (m, 8 H, HON-CH_2 and ArNH-CH_2), 3.153 (t, J = 5.7 Hz, 4 H, $NHCH_2$), 2.748 (t, J = 7.1 Hz, 4 H, $COCH_2$), 2.442 (t, J = 6.5 Hz, 4 H, $COCH_2$), 2.082 (s, 3 H, $OCOCH_3$), and 1.2–1.8 ppm (m, 18 H, aliphatic CH); IR (KBr): ν 3315 (NH), 1626.5 (CONH and CONOH), and 1589 cm^{-1} (Ar); UV (aqueous methanol): λ_{max}, 470 and 340 nM (ϵM^{cm} 15,200 and 4,870, respectively).

NBD-DFO fluorescence spectra and quenching by metal ions. NBD-DFO fluorescence spectra were determined in buffered saline (150 mM NaCl, 10 mM HEPES, pH 7.4), with 475-nm excitation and monitoring of fluorescence intensity over a range of 500–600 nm (maximal emission at 548 nm). The fluorescence measurements were carried out in 1-ml plastic cuvettes (Elkay Ultra-Vu), using a SPEX Fluorolog II (DM1B) with slit widths set to 1 mm. Quenching of NBD-DFO (2 μM NBD-DFO in buffered saline) by Fe(III) was detected after additions of $FeCl_3$ aliquots from 1 mM methanolic solutions and monitoring of fluorescence intensity. The final methanol concentration was <0.3%. NBD-DFO-Fe^{3+} complex was dissociated by lowering of the pH to <2 with either TCA or HCl and addition of EDTA to a final concentration of 500 μM.

The effects of other metal ions on NBD-DFO fluorescence were measured in a similar fashion, using $CuNO_3$, $ZnCl_2$, $MnCl_2$, $MgCl_2$, or $CaCl_2$ methanolic stock solutions. All salts except $CuNO_3$ were directly soluble in methanol (at 20 mM). Pure copper powder (Merck) was dissolved in nitric acid, and methanol was added to yield a 5% nitric acid final concentration. The metal-NBD-DFO mixtures were allowed to incubate 30 min in Eppendorf tubes before monitoring of fluorescence. Quenching due to the metal ions was analyzed by Stern-Volmer plots.

Determination of DFO and NBD-DFO iron-binding efficiency and partition coefficient. The relative iron-binding efficiencies of DFO and NBD-DFO were determined in aqueous methanol (0.1 N sodium acetate/methanol) by measuring the fluorescence of NBD-DFO in the presence of equimolar mixtures of DFO and Fe^{3+}. Equimolar amounts of NBD-DFO and $FeCl_3$ were equilibrated in methanolic solution for 1 hr, and the fluorescence spectra were recorded (excitation wavelength, 468 nm; emission range, 500–580 nm) and compared with those of similar mixtures lacking Fe(III). Partition coefficients were determined by equilibration of either the free chelator or the preformed iron-chelator complexes between equal volumes of *n*-octanol and buffered saline (150 mM NaCl, 10 mM HEPES, pH 7.4) for 4 hr. The NBD-DFO concentrations in each phase were determined by absorbance in the 470-nm range or by fluorescence, as described above. The concentrations of NBD-DFO-Fe complexes were determined by visible-wavelength spectroscopy only, and those of DFO were determined by addition of excess Fe(III) and measurement of the ferric complex absorbance at 430 nm. Partition coefficients were calculated as ratios of the compound concentrations in *n*-octanol versus saline.

Parasite cultures and bioassay of drug antimalarial activity. *P. falciparum* strains used in this study, Brazilian strain ItG2G1 (obtained from L. H. Miller) and drug-resistant strains FCR-3 (Gambian, provided by J. B. Jensen) and K1, were grown in culture flasks of human erythrocytes by a modified version of Trager and Jensen's method (26) published elsewhere (27). The antimalarial activity of iron chelators was assayed by addition of chelators from concentrated stock solutions (in DMSO) to microcultures (24-well, Nunclon) containing infected red cells (2.5% hematocrit and 2% parasitemia). The cultures were synchronized by incubation in 300 mM L-alanine, 10 mM Tris·HCl. After incubation with drug for 24 hr, the cells were supplemented with 6 μCi/ml [^{3}H]hypoxanthine, and parasite growth was assessed 24 hr later by harvesting of the labeled cells onto glass fiber filters (Tamar Inc., Jerusalem) and counting of the radioactivity.

Uptake of NBD-DFO into normal and infected erythrocytes. NBD-DFO uptake was assessed under parasite growth conditions described above. Trophozoites and noninfected red cells were obtained from synchronized cultures and separated by the alanine/Percoll method described elsewhere (28). Percoll was removed by repeated washes of the cells in buffer (150 mM NaCl, 10 mM HEPES, 50 mM sucrose, pH 7.4) containing step-wise decrease in L-alanine concentration (1.5%, 0.75%, 0.3%, and 0%). Cells were then resuspended in RPMI medium supplemented with 10% human plasma and NBD-DFO was added from concentrated stock solution in DMSO (<0.1% DMSO final concentration). Suspensions of 0.5% of 1.2% hematocrit were incubated in culture flasks, and 6 and 12 ml, respectively, were sampled at each time point. The cells were washed in ice-cold saline buffer containing 50 mM sucrose, and NBD-DFO influx was monitored by measuring fluorescence inside cell lysates.

Uptake of ^{59}Fe-chelator complexes. Iron-chelator complexes were preformed by the addition of $^{59}Fe(III)Cl_3$ (Amersham) to concentrated stock solutions containing NBD-DFO and DFO in DMSO and incubation at room temperature for 1 hr. To initiate the flux, radioactive complexes were added to suspensions of noninfected and infected red cells that had been prewarmed to 37° in saline buffer (150 mM NaCl, 10 mM HEPES, 50 mM sucrose, 20 mM glucose, supplemented with 100 μM sodium citrate and 10% bovine serum albumin to avoid precipitation of ferric iron). Suspensions of 1.2 ml at 20% hematocrit, 20 μg/ml chelator, and 5 μM ^{59}Fe (final concentrations) were incubated at 37°, with gentle shaking, in 15-ml plastic test tubes (Sarstedt). For each time point, two 75-μl aliquots were centrifuged at 2000 × *g* for 1 min, supernatants were removed, and cell pellets (15 μl) were washed in 12 ml of ice-cold saline buffer containing 50 mM EDTA. Radioactive pellets were kept on ice until lysis in distilled water and transfer to scintillation vials for counting of γ emission (700–1250 KeV). The cell number in each sample was determined from hemoglobin absorption at 410 nm (28).

Chelation of iron from infected red cells. Extraction of chelatable iron from noninfected and infected red cells (trophozoites, from Percoll gradients) was carried out on red cell suspensions (20% hematocrit) by incubation for 3–4 hr at 37° in saline buffer containing 50 mM sucrose, 25 mM glucose, and NBD-DFO at 2–10 μg/ml. Control samples were incubated under identical conditions without NBD-DFO. After centrifugation at 1000 × *g* for 5 min, cell pellets were washed in 12 ml of ice-cold buffer and lysed in 750 μl of distilled water. Lysates were sampled for hemoglobin measurements (410 nm) and then trans-

MOL PHARM
MOLECULAR PHARMACOLOGY
aspet
Downloaded from molpharm.aspetjournals.org at Universidade do Estado do Rio de Janeiro on December 4, 2012

ferred to Eppendorf tubes, where they were protein precipitated by addition of ice-cold TCA (5% final concentration). The TCA-soluble material was removed and stored at 4° in Eppendorf tubes for measurements of fluorescence intensity. Chelated iron was released by addition of EDTA, as shown below.

Results

NBD-DFO fluorescent properties. Addition of NBD label to DFO imparts fluorescent properties to the free carrier. Excitation at 475 nm and monitoring of the emission spectra over a range of 500–600 nm reveal a single peak at 548 nm, which is quenched upon loading of the carrier with ferric iron (Fig. 2A). The conclusion that quenching resulted from binding of the iron was based on the fact that the fluorescence of NBD derivatives of various amino acids (e.g., NBD-alanine and NBD-taurine) was not affected by addition of similar concentrations of iron salts. Moreover, at acid conditions (pH <5) quenching of NBD-DFO by iron was fully retained, and at physiological pH addition of EDTA did not change the fluorescence intensity of the NBD-DFO-Fe complex (results not shown). However, when pH was lowered with either HCl or TCA, addition of excess EDTA fully reversed the quenching, indicating that it competed with the hydroxamate ligand and removed the bound iron from NBD-DFO (Fig. 2B). This property provided the analytical basis for assessing the NBD-DFO-mediated sequestration of Fe^{3+} from intracellular sources.

Effects of metal ions on NBD-DFO fluorescence. In order for NBD-DFO to serve as a specific probe for ferric iron, it had to be established to what extent other biologically relevant metal ions present in host cells and body fluids can affect NBD-DFO fluorescence. For this reason, we tested the capacity of various divalent cations, such as Ca(II), Zn(II), Cu(II), Mg(II), and Mn(II), to act as fluorescence quenchers. Besides Fe(III), only Cu(II) produced significant quenching (Fig. 3). Ca^{2+} and Mg^{2+} had no effect on fluorescence signal, and Zn^{2+} and Mn^{2+} had marginal quenching activity at concentrations 100–200-fold higher than that of Fe^{3+} (results not shown). However, after addition of TCA (2.5% final) to 2 μM NBD-DFO and 10 μM Cu^{2+} ions, quenching by the metal ion was completely abolished (Fig. 3). These observations demonstrate that it is possible to experimentally discern NBD-DFO-bound Fe(III) from NBD-DFO-bound Cu(II).

Dose response of NBD-DFO versus DFO. Exposure of *P. falciparum* to DFO and NBD-DFO results in inhibition of parasite growth (Fig. 4). Antimalarial activities of NBD-DFO and DFO, compared at their IC_{50} values (5 ± 0.62 and 26 ± 5 μM, respectively), show that NBD-DFO is 5–6-fold more potent than DFO. NBD-DFO was also tested for its inhibitory effect in several different strains of *P. falciparum* and was found to be effective against both chloroquine-sensitive strain ItG2G1 and highly drug-resistant strains FCR-3 and K1 (Table 1).

Correlation of biological effects with physicochemical properties. Iron-binding properties and lipid solubilities of

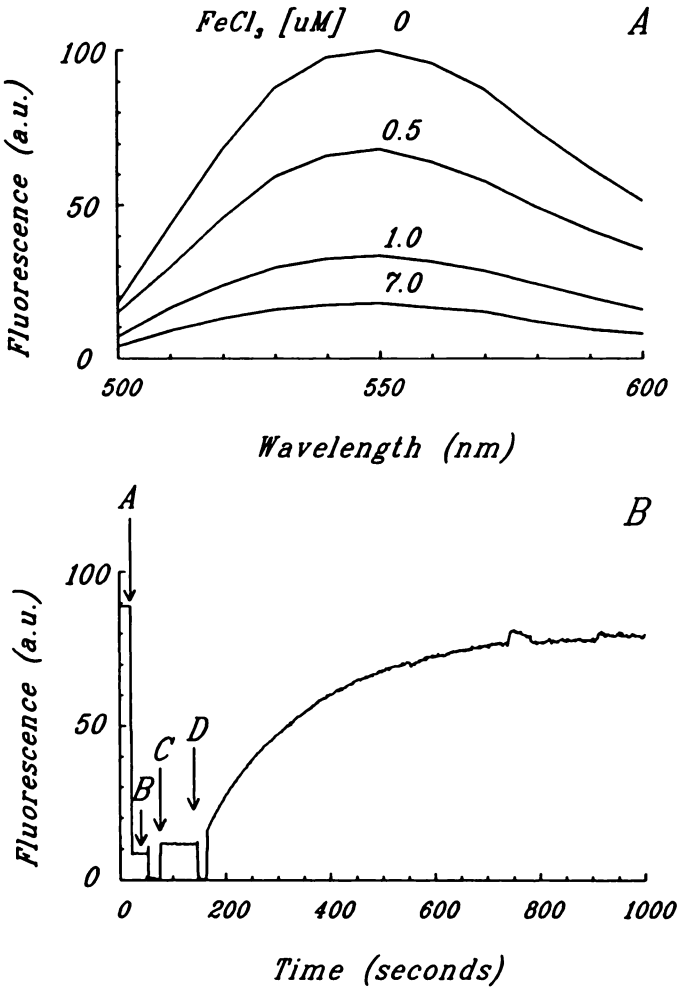

Fig. 2. Fluorescence properties of NBD-DFO and its ferric iron complex. A, Fluorescence emission spectra (475-nm excitation) of free NBD-DFO (1 μM) in buffer containing 150 mM NaCl and 10 mM HEPES, pH 7.4, and in the presence of 0.5, 1, or 7 equivalents of $FeCl_3$. B, Iron binding to NBD-DFO. Fluorescence intensity is of free NBD-DFO ligand (*A*), after addition of $FeCl_3$ (7 μM final concentration) (*B*), after acidification with HCl (0.1 M final concentration, pH <3) (*C*), and after addition of EDTA (500 μM final concentration) (*D*). *Arrows*, time points of additions. The monitoring and measurements of fluorescence intensity are described in Materials and Methods.

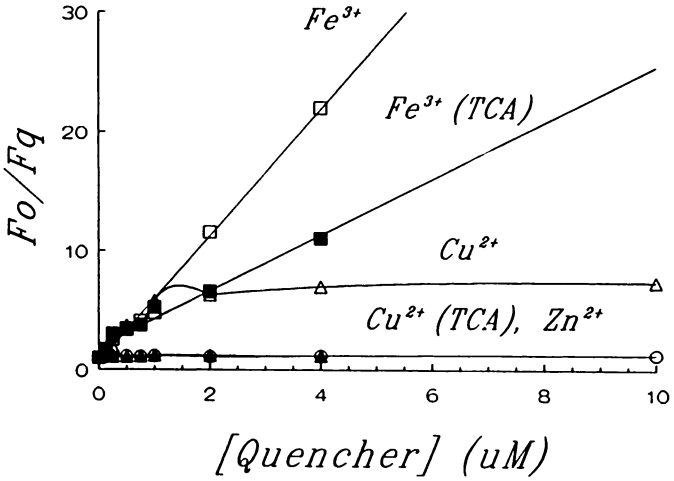

Fig. 3. NBD-DFO fluorescence quenching by metal ions. The quenching of NBD-DFO fluorescence was assayed by addition of different salts to a 2 μM solution of NBD-DFO in pH 7.4 buffer and measurement of the fluorescence intensity at each concentration of metal ion quencher shown. The fluorescence intensity in buffer alone (F_o) relative to that in the presence of metal ion quencher (F_q) is plotted as a function of quencher concentration. Stern-Volmer quenching constants (K_q) obtained from the slopes of plotted data are Fe^{3+}, $K_q = 5.28 \pm 0.175 \times 10^6$ (□); Cu^{2+}, $K_q = 2.57 \pm 0.413 \times 10^6$ (△); and Zn^{2+}, $K_q = 4 \pm 2 \times 10^4$ (○); and, in buffer containing 2.5% TCA, pH <2, Fe^{3+}, $K_q = 3.71 \pm 0.64 \times 10^6$ (■); and Cu^{2+} (▲), K_q could not be determined with accuracy.

MOL PHARM
MOLECULAR PHARMACOLOGY
aspet
Downloaded from molpharm.aspetjournals.org at Universidade do Estado do Rio de Janeiro on December 4, 2012

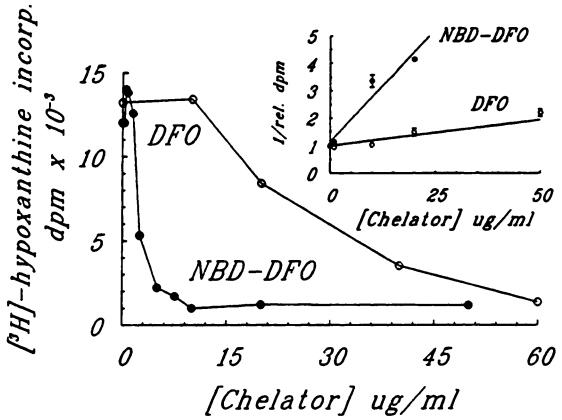

Fig. 4. Effect of iron chelators on *in vitro* parasite growth. Growth inhibition by NBD-DFO and desferal was assayed over a 48-h exposure period, as described in Materials and Methods. *Inset*, Dixon plot shows regression lines of four independent experiments. IC_{50} (μM) (mean ± SD): desferal, 26 ± 5; NBD-DFO, 5 ± 0.62.

TABLE 1

Antimalarial activity of DFO and its NBD analog in different *P. falciparum* strains

The antimalarial activity was assessed over a 48-hr period of exposure, including a 24-hr period of [³H]hypoxanthine incorporation into nucleic acids (see Materials and Methods). K1 and FCR-3 represent chloroquine-resistant strains of *P. falciparum*, whereas ItG2G1 represents a sensitive strain. Values are mean ± standard deviation.

Parasite strain	IC_{50}	
	DFO	NBD-DFO
	μg/ml	
ItG2G1	31 ± 11	3 ± 1
K1	12 ± 6	3 ± 1
FCR-3	41 ± 10	5 ± 1

TABLE 2

Antimalarial activity and physicochemical properties of DFO and NBD-DFO

For determination of the tabulated values of iron binding and partition coefficients (P_{coeff}), see Materials and Methods. IC_{50} values are for the ItG2G1 strain, measured as described in Materials and Methods and as shown in Fig. 4 and Table 1, but from two independent sets of experiments (mean ± standard deviation).

Compound	Fe binding (relative)	P_{coeff}	IC_{50}
			μg/ml
DFO	1.0	<0.1	26 ± 5
NBD-DFO	1.5	5 ± 1	5 ± 1
NBD-DFO-Fe		<1	—[a]

[a] —, No detectable inhibition of growth with 1:1 NBD-DFO-Fe complexes.

NBD-DFO, DFO, and their ferric complexes were determined (Table 2). Although the relative Fe(III)-binding efficiencies of the uncomplexed NBD-DFO versus DFO were found to be very close, namely 3:2, the partition coefficient of NBD-DFO in *n*-octanol/saline was 5, which is at least 40–50-fold higher than that of DFO. The partition coefficient of the preformed NBD-DFO-Fe complex was 1.5, which is considerably lower than that of the free NBD-DFO.

NBD-DFO and NBD-DFO-^{59}Fe(III) uptake into infected red cells. In view of the demonstrable antimalarial activity and enhanced lipophilicity of NBD-DFO, we studied the permeability of red cells to the free ligand. In order to accomplish this, we took advantage of the fluorescence of the compound and our ability to detect it in red cell lysates after TCA precipitation. Fig. 5 shows results of NBD-DFO uptake after exposure of noninfected and infected erythrocytes for various time intervals. The uptake is highly selective for infected cells, with no detectable uptake found in noninfected red cells obtained from the same cultures as the 100% parasitized erythrocytes. Uptake showed similar pseudo-first-order kinetics in two independent experiments at different concentrations of NBD-DFO. Initial rates were the same at both concentrations, with small differences being apparent in the final level of uptake. At the high concentration (experiment 1) maximum uptake observed was 70% of the amount expected at equilibrium, whereas at the lower concentration (experiment 2) the uptake maximum was in agreement with the equilibrium value.

The relatively low partition coefficient of NBD-DFO-Fe(III), compared with NBF-DFO, was correlated with its poor penetration into red cells (normal or infected), as measured by NBD-DFO-^{59}Fe uptake. The level of uptake attained after 8 hr of incubation with red cell suspensions was essentially the same as that of control (<5% of the extracellular concentration of complexed ^{59}Fe) (Fig. 6).

Extraction of chelatable iron from infected red cells. Because NBD-DFO can specifically complex Fe(III), we examined the possibility that the degree of iron chelation in infected red cells might be considerably higher than that in noninfected red cells. As shown in Fig. 7, the amount of iron

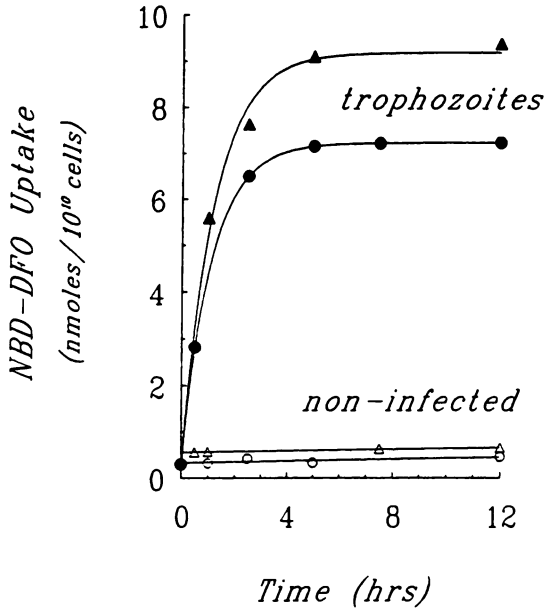

Fig. 5. Uptake of NBD-DFO into infected and noninfected erythrocytes. The uptake of NBD-DFO into normal red cells (open symbols) and red cells infected at the trophozoite stage (*closed symbols*) was measured by addition of NBD-DFO to cell suspensions in growth medium and then monitoring of the fluorescence in cell lysates at the time points indicated, as described in Materials and Methods. The uptake values plotted (nmol/10^{10} cells) were calculated from total fluorescence inside cells after lysis, TCA addition (with or without EDTA), and references to an NBD-DFO standard curve. The number of cells was determined by hemoglobin absorption at 410 nm. Results are shown for chelator uptake in two experiments; in experiment 1 (*triangles*) the hematocrit and NBD-DFO concentrations, respectively, were 0.5% and 13 μM and in experiment 2 (*circles*), 1.2% and 7 μM. Parasitemia in both experiments was >95%. The uptake of NBD-DFO into infected cells was analyzed by first-order rate kinetics using the ENZFIT program. The lines represent the nonlinear regression fits to the experimental points, using as the zero time value the background value obtained with noninfected cells; the $t_{1/2}$ of uptake was 45 ± 10 min.

MOL PHARM
MOLECULAR PHARMACOLOGY
aspet
Downloaded from molpharm.aspetjournals.org at Universidade do Estado do Rio de Janeiro on December 4, 2012

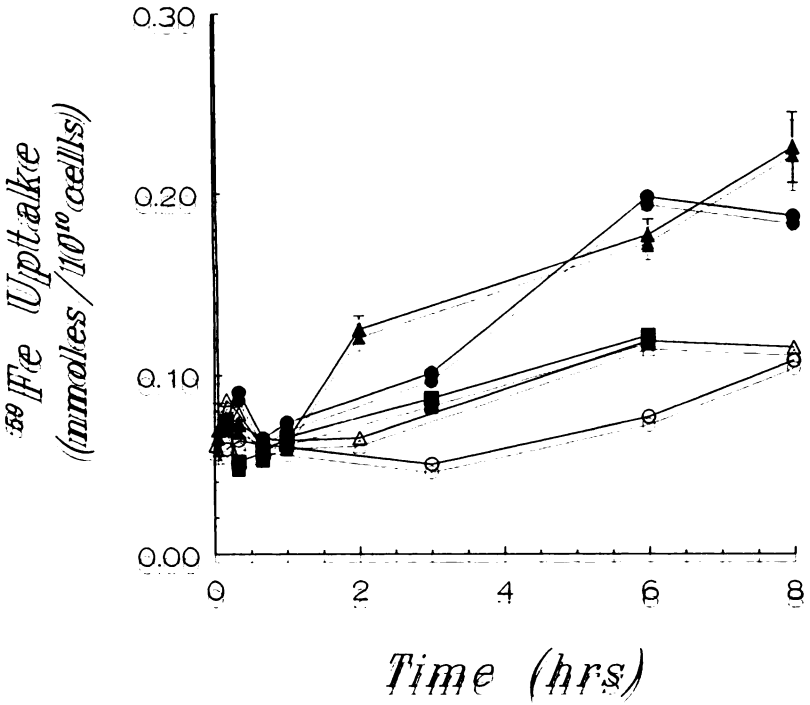

Fig. 6. Uptake of ^{59}Fe-chelator complexes. ^{59}Fe-chelator complexes were preformed at 1:5 ratio by addition of ^{59}Fe(III)Cl$_3$ to either NBD-DFO or desferal in DMSO. The radioactive mixtures were then added to normal (*open symbols*) and 70% infected (*closed symbols*) red cell suspensions to give 20% hematocrit, 20 μg/ml chelator, and 5 μM Fe^{3+} (final concentrations). The radioactivity in cell pellets of duplicate samples was counted at the time points indicated, and the values were converted to nmol/10^{10} cells. Uptake is shown for NBD-DFO (*triangles*), desferal (*circles*), and DMSO control (*squares*).

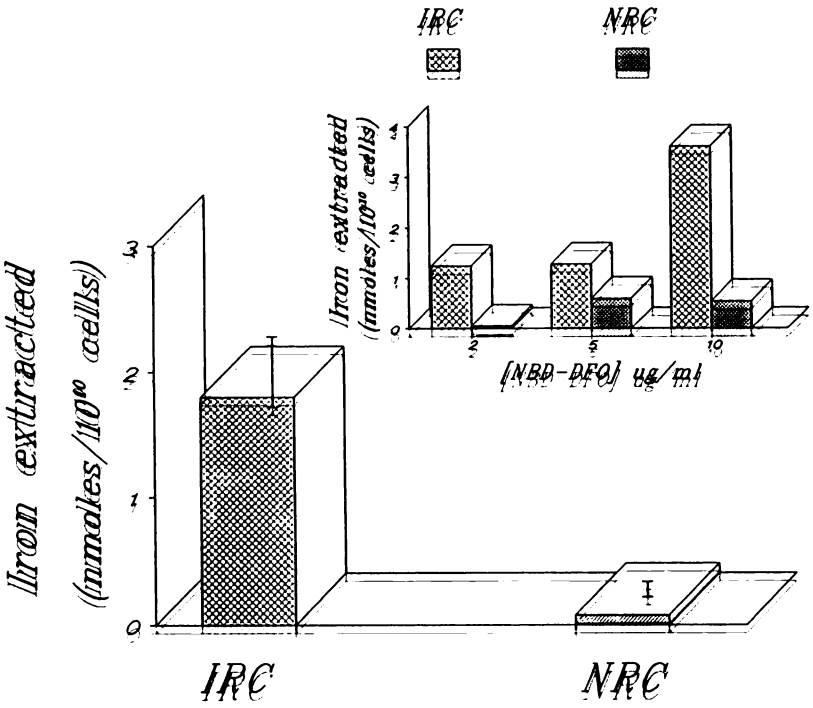

Fig. 7. Extraction of chelatable iron from normal (*NRC*) versus infected red cells (*IRC*). The amount of chelatable iron extracted from normal and 100% infected red cells was assessed after treatment of cell suspensions with 2 μg/ml NBD-DFO and measurement of the fluorescence intensity in cell lysates. Iron bound to the chelator was released with 500 μM EDTA, and the values represent conversion of absolute change in fluorescence intensity before and after EDTA addition to nmol of iron extracted/10^{10} cells. Cells were obtained from Percoll gradients and incubated at 20% hematocrit with NBD-DFO for 3 hr, as described in Materials and Methods. Mean and standard deviation represent values obtained from three experiments. *Inset*, amount of iron extracted using three different concentrations of NBD-DFO.

extracted from 100% parasitized red cells using 2.8 μM NBD-DFO was approximately 2 nmol/10^{10} cells, approximately equivalent to an intracellular concentration of chelatable iron of 2 μM (without taking into consideration compartmentalization, the water-available space of infected cells, which could not be accurately determined). In contrast, the exposure of noninfected red cells to the same NBD-DFO concentration resulted in 20-fold lower iron extraction. In order to determine how much of this difference is actually attributed to greater accessibility of NBD-DFO to the interior of infected red cells, extractions were performed at three different NBD-DFO concentrations. At an exposure of 10 μg/ml, the total amount of NBD-DFO in noninfected red cells was approximately equal to the amount of probe in infected red cells exposed to 2 μg/ml. However, a comparison of the total iron extracted clearly shows 2–3-fold higher chelatable iron in the infected red cells (Fig. 7, *inset*).

Discussion

Previous studies of iron chelation and inhibition of *P. falciparum* growth showed that the major source of Fe^{3+} used for intraerythrocytic parasite growth resides with components of the infected cell (11, 20, 21) and not in the serum. The possible

MOL PHARM
MOLECULAR PHARMACOLOGY
aspet
Downloaded from molpharm.aspetjournals.org at Universidade do Estado do Rio de Janeiro on December 4, 2012

MOL PHARM

MOLECULAR PHARMACOLOGY

intracellular donors of Fe(III) are hemoglobin degradation/oxidation products (22–24), intraerythrocytic residual ferritin, or parasite-derived enzymes or siderophores. Although preliminary experiments with horse ferritin indicated that reversed siderophores can indeed sequester Fe^{3+} from this source,[1] the relevant Fe^{3+} targets of these chelator remain to be identified.

These findings regarding sensitive Fe^{3+} pools in infected erythrocytes and the ostensible differences in permeability found in membranes of parasitized cells, compared with normal cells (29), led us to the design of the Fe^{3+} chelator NBD-DFO (Fig. 1), which is selectively admitted by infected cells (Fig. 5), where it sequesters Fe^{3+}. NBD-DFO meets the major criteria of antimalarial agents, which are efficacy as reflected in IC_{50} concentrations measured over one to two generations of parasites exposed to drug (Table 2), inhibitory power on *P. falciparum* strains with different drug sensitivities (Table 1), and, most importantly, a high degree of selectivity for target cells (i.e., infected versus noninfected erythrocytes). The observed temperature dependence of uptake of various reversed siderophores into infected cells is consistent with a simple diffusion process (21).[2] An analogous approach aimed at increasing the lipophilicity of DFO was applied to "lazaroids" for treating ischemic conditions (30).

The introduction of the NBD residue at the amino-terminal group of DFO was chosen because that group was shown by X-ray crystallography not to participate in iron binding (31). The amino-terminal-coupled NBD group confers major advantages to NBD-DFO, relative to DFO. While fully preserving the Fe(III)-binding properties of the parent DFO, addition of NBD demonstrably enhances the hydrophobicity of the molecule and reduces its basicity, thus minimizing protonation of the molecule at physiological pH. Consequently, partitioning of NBD-DFO into lipophilic phases is enhanced and permeation across cellular membranes is facilitated, with the additional bonus of increased selectivity for parasitized erythrocytes. Moreover, NBD provides the hydroxamate binding moiety with a fluorescent marker than enables specific assay of Fe^{3+} and monitoring of its intracellular pathways in a variety of cell systems. This is based on the fact that, as Fe^{3+} binds to NBD-DFO, marked quenching of the NBD group ensues because of the proximity of the metal ion to the fluorophor. The addition of excess EDTA in acidic environment dissociates the NBD-DFO-Fe^{3+} complex and restores the fluorescence properties of the probe.

The highly selective permeation of NBD-DFO across membranes of infected red cells surpasses that of DFO and correlates well with the demonstrable alterations in permselectivity (28, 29) and lipid composition (32) of the membrane of infected cells. The level of NBD-DFO uptake into infected cells was found to be 20-fold higher than that into noninfected red cells after 40–50 min of incubation (Fig. 5), whereas DFO, on the other hand, showed only 3 times higher permeation in parasitized cells after 4 hr of incubation (19). The enhanced antimalarial activity of NBD-DFO, relative to DFO (Fig. 4), is in agreement with our earlier findings on reversed siderophores, whose antimalarial activity was shown to be highly correlated with the lipophilicity of the synthetic ferrichrome (21). The antimalarial activity of NBD-DFO can be attributed to chelator-mediated Fe^{3+} sequestration from infected erythrocytes. However, the fact that the iron-NBD-DFO complex has a considerably lower partition coefficient than the free chelator (Table 2) might explain why the iron-bound NBD-DFO that is formed inside parasitized cells after uptake of NBD-DFO is retained inside the infected red cell. In previous studies based on DFO (21, 33), it was claimed that complexation of Fe(III) to the chelator eliminated the intracellular inhibitory activity of DFO on parasitized cells. As shown in this work for NBD-DFO-Fe^{3+}, neutralization of such activity could have resulted from the formation of membrane-impermeant (or poorly permeant) chelator-Fe^{3+} complexes. However, irrespective of the mode of action of NBD-DFO as an antimalarial agent in *in vitro* studies with *P. falciparum*-infected human erythrocytes, its improved biological and spectroscopic properties, relative to DFO, warrant its application as an antimalarial agent *in vivo* in studies with animal models, and work on this is in progress. In general, the specific iron chelator properties of NBD-DFO and its unique spectroscopic properties open the possibility of assessing the intracellular pathways of iron metabolism in both normal and pathological states and studying the effects of other iron chelators and siderophores on living systems.

Acknowledgments

The excellent assistance of Mrs. Hava Glickstein in the initial stages of this study is kindly acknowledged.

References

1. Peters, W. The problem of drug resistance in malaria. *Parasitology* **90**:705–715 (1985).
2. Clyde, D. F. Recent trends in the epidemiology and control of malaria. *Epidemiol. Rev.* **9**:219–228 (1987).
3. Harvey, P. W. J., P. F. Heywood, M. C. Nesheim, K. Galme, M. Zegans, J. P. Habicht, L. S. Stephenson, K. L. Radimer, B. Brabin, K. Forsyth, and M. P. Alpers. The effect of iron therapy on malarial infection in Papua New Guinea schoolchildren. *Am. J. Trop. Med. Hyg.* **40**:12–18 (1989).
4. Oppenheimer, S. J., F. D. Gibson, S. B. Macfarlane, J. B. Moody, C. Harrison, A. Spencer, and O. Bunari. Iron supplementation increases prevalence and effects of malaria: report on clinical studies in Papua New Guinea. *Trans. R. Soc. Trop. Med. Hyg.* **80**:603–612 (1986).
5. Murray, M. J., A. B. Murray, and C. J. Murray. The adverse effects of iron repletion on the course of certain infections. *Br. Med. J.* **2**:113–115 (1978).
6. Aremu, C. Y. Changes in serum transferrin and iron concentrations in humans suffering from malaria with parasitemia. *Ann. Trop. Med. Parasitol.* **83**:517–520 (1989).
7. Raventos-Suarez, C., S. Pollack, and R. L. Nagel. *Plasmodium falciparum*: inhibition of *in vitro* growth by desferrioxamine. *Am. J. Trop. Med. Hyg.* **31**: 919–922 (1982).
8. Heppner, G., P. E. Hallaway, G. J. Kontoghiorghes, and J. W. Eaton. Antimalarial properties of orally active iron chelators. *Blood* **72**:358–361 (1988).
9. Stahel, E., D. Mazier, A. Guillouzo, F. Miltgen, I. Landau, S. Mellouk, R. L. Beaudoin, P. Langlois, and M. Gentilini. Iron chelators: *in vitro* inhibitory effect on the liver stage of rodent and human malaria. *Am. J. Trop. Med. Hyg.* **39**:236–240 (1988).
10. Fritsch, G., J. Treumer, D. T. Spira, and A. Jung. *Plasmodium vinckei*: suppression of mouse infections with desferrioxamine B. *Exp. Parasitol.* **60**: 171–178 (1985).
11. Hershko, C., and T. E. Peto. Deferoxamine inhibition of malaria is independent of host iron status. *J. Exp. Med.* **168**:375–387 (1988).
12. Pollack, S., R. N. Rossan, D. E. Davidson, and A. Escajadillo. Desferrioxamine suppresses *Plasmodium falciparum* in Aotus monkeys. *Proc. Soc. Exp. Biol. Med.* **184**:162–169 (1987).
13. Barry, M., D. M. Flynn, E. A. Letsky, and R. A. Risdon. Long-term chelation therapy in thalasseaemia major: effect on liver iron concentration, liver histology and clinical progress. *Br. Med. J.* **2**:16–20 (1974).
14. Hershko, C., and D. J. Weatherall. Iron-chelating therapy. *Crit. Rev. Clin. Lab. Sci.* **26**:303–345 (1988).
15. Wolfe, L. C., R. J. Nicolosi, M. M. Renaud, J. Finger, M. Hegsted, H. Peter, and D. Nathan. A non-human model for study of oral iron chelators. *N. Engl. J. Med.* **312**:1600–1610 (1989).
16. Borgna-Pignatti, C., P. de Stafano, and A. M. Borglia. Visual loss in patient on high-dose subcutaneous desferrioxamine. *Lancet* **1**:681–689 (1984).
17. Blake, D. R., P. Winyard, J. Lunec, A. Williams, P. A. Good, S. J. Crewes, J. M. C. Gutteridge, D. Rowley, B. Halliwell, A. Cornish, and R. C. Hider. Cerebral and ocular toxicity induced by desferrioxamine. *Q. J. Med.* **56**:345–

[1] S. D. Lytton, J. Libman, A. Shanzer, and Z. I. Cabantchik, unpublished observations.

[2] S. D. Lytton, J. Libman, A. Shanzer, and Z. I. Cabantchik, manuscript in preparation.

aspet

Downloaded from molpharm.aspetjournals.org at Universidade do Estado do Rio de Janeiro on December 4, 2012

355 (1985).
18. Porter, J. B., S. Mervyn, E. R. Jawson, C. A. Huehns, C. East, and J. W. P. Hazell. Desferrioxamine ototoxicity: evaluation of risk factors in thalassaemic patients and guidelines for safe dosage. *Br. J. Haematol.* **73:**403–409 (1989).
19. Fritsch, G., and A. Jung. ^{14}C-Desferrioxamine B: uptake into erythrocytes infected with *Plasmodium falciparum*. *Z. Parasitenkd.* **72:**709–713 (1986).
20. Peto, T. E., and J. L. Thompson. A reappraisal of the effects of iron and desferrioxamine on the growth of *Plasmodium falciparum in vitro*: the unimportance of serum iron. *Br. J. Haematol.* **63:**273–280 (1986).
21. Shanzer, A., J. Libman, S. D. Lytton, H. Glickstein, and Z. I. Cabantchik. Reversed siderophores act as antimalarial agents. *Proc. Natl. Acad. Sci. USA*, **88:**6585–6589 (1991).
22. Goldberg, D. E., A. F. G. Slater, A. Cerami, and G. B. Henderson. Hemoglobin degradation in the malaria parasite *Plasmodium falciparum*: an ordered process in a unique organelle. *Proc. Natl. Acad. Sci. USA* **87:**2931–2935 (1990).
23. Bullen, J. J., and E. Griffiths. *Iron and Infection: Molecular, Physiological and Clinical Aspects*. John Wiley and Sons Ltd., London, 1–27 (1987).
24. Slater, A. F. G., W. J. Swiggard, B. R. Orton, W. D. Flitter, D. E. Goldberg, A. Cerami, and G. B. Henderson. An iron-carboxylate bond links the heme units of malaria pigment. *Proc. Natl. Acad. Sci. USA* **88:**325–329 (1991).
25. Ghosh, B. P., and M. W. Whitehouse. 7-Chloro-4-nitro-benzo-2-oxa-1,3-diazole: a new fluorogenic reagent for amino acids and other amines. *Biochem. J.* **108:**155–156 (1968).
26. Trager, W., and J. B. Jensen. Continuous culture of human malaria parasites. *Science (Washington D. C.)* **193:**673–675 (1976).
27. Jensen, J. B. Concentration from continuous culture of erythrocytes infected with trophozoites and schizonts of *Plasmodium falciparum*. *Am. J. Trop. Med. Hyg.* **27:**1274–1276 (1978).
28. Kutner, S., W. V. Breuer, H. Ginsburg, S. B. Aley, and Z. I. Cabantchik. Characterization of permeation pathways in the plasma membrane of human erythrocytes infected with early stages of *Plasmodium falciparum*: association with parasite development. *J. Cell. Physiol.* **125:**521–527 (1985).
29. Cabantchik, Z. I. Altered membrane transport of malaria-infected erythrocytes: a possible pharmacologic target. *Blood* **74:**1464–1471 (1989).
30. Braughler, J. M., P. S. Burton, R. L. Chase, J. F. Pregenzer, J. Jacobsen, F. J. Van Doornik, J. M. Tustin, D. E. Ayer, and G. L. Bundy. Novel membrane localized iron chelators as inhibitors of iron-dependent lipid peroxidation. *Biochem. Pharmacol.* **37:**3853–3860 (1988).
31. Hossain, M. B., M. A. F. Jalal, and D. Van der Helm. The structure of ferrioxamine D_1-ethanol-water. *Acta Crystallogr. C* **42:** 1305–1310.
32. Maguire, P. A., and I. W. Sherman. Phospholipid composition, cholesterol content and cholesterol exchanges in *Plasmodium falciparum*-infected red cells. *Mol. Biochem. Parasitol.* **38:**105–112 (1990).
33. Whitehead, S., and T. E. A. Peto. Stage-dependent effect of deferoxamine on growth of *Plasmodium falciparum in vitro*. *Blood* **76:**1250–1255 (1990).

Send reprint requests to: Z. Ioav Cabantchik, Department of Biological Chemistry, Institute of Life Sciences, Hebrew University, Jerusalem, Israel 91904.

MOL PHARM
MOLECULAR PHARMACOLOGY
aspet
Downloaded from molpharm.aspetjournals.org at Universidade do Estado do Rio de Janeiro on December 4, 2012